



# Fatal Pertussis in the Neonatal Mouse Model Is Associated with Pertussis Toxin-Mediated Pathology beyond the Airways

Karen M. Scanlon, Yael G. Snyder,\* Ciaran Skerry, Nicholas H. Carbonetti

Department of Microbiology and Immunology, University of Maryland School of Medicine, Baltimore, Maryland, USA

**ABSTRACT** In infants, *Bordetella pertussis* can cause severe disease, manifested as pronounced leukocytosis, pulmonary hypertension, and even death. The exact cause of death remains unknown, and no effective therapies for treating fulminant pertussis exist. In this study, a neonatal mouse model of critical pertussis is characterized, and a central role for pertussis toxin (PT) is described. PT promoted colonization, leukocytosis, T cell phenotypic changes, systemic pathology, and death in neonatal but not adult mice. Surprisingly, PT inhibited lung inflammatory pathology in neonates, a result which contrasts dramatically with observed PT-promoted pathology in adult mice. Infection with a PT-deficient strain induced severe pulmonary inflammation but not mortality in neonatal mice, suggesting that death in these mice was not associated with impaired lung function. Dissemination of infection beyond the lungs was also detected in neonatal mice, which may contribute to the observed systemic effects of PT. We propose that it is the systemic activity of pertussis toxin and not pulmonary pathology that promotes mortality in critical pertussis. In addition, we observed transmission of infection between neonatal mice, the first report of *B. pertussis* transmission in mice. This model will be a valuable tool to investigate causes of pertussis pathogenesis and identify potential therapies for critical pertussis.

**KEYWORDS** *Bordetella pertussis*, pertussis toxin, leukocytosis, neonatal infection, disseminated infection

Pertussis, caused by the bacterial pathogen *Bordetella pertussis*, remains a major public health concern, as incidence continues to increase in many countries (1). Pertussis is typically characterized by episodes of severe and persistent paroxysmal coughing (2). Although pertussis vaccines are in widespread use, the first dose is not administered until 2 months of age or later, leaving very young infants susceptible to pertussis (3, 4). In infants the disease can be particularly severe, requiring hospital intensive care (5, 6). Pneumonia, pronounced leukocytosis, hypoxia, and pulmonary hypertension are common manifestations of severe pertussis disease in infants (5–8), and almost all pertussis fatalities are in this age group (4, 8, 9). Autopsy studies of lungs from fatal pertussis cases commonly describe severe necrotizing bronchitis, pneumonia, and edema, as well as pronounced leukocytosis visible in pulmonary vasculature (6, 10). However, few, if any, effective therapies for treatment of critical pertussis exist (3, 8, 11). It is unclear why pathogenesis of pertussis disease is different in young infants, but it is well known that the immune system in infants is not equivalent to that in older children and adults (12–14), potentially leaving infants susceptible to exacerbated infection and disease.

Previous studies showed that neonatal (6-day-old) BALB/c mice were susceptible to lethal *B. pertussis* infection after intranasal inoculation with doses ( $10^4$  to  $10^5$  CFU) that

Received 15 May 2017 Returned for  
modification 11 July 2017 Accepted 3  
August 2017

Accepted manuscript posted online 7  
August 2017

**Citation** Scanlon KM, Snyder YG, Skerry C,  
Carbonetti NH. 2017. Fatal pertussis in the  
neonatal mouse model is associated with  
pertussis toxin-mediated pathology beyond  
the airways. *Infect Immun* 85:e00355-17.  
<https://doi.org/10.1128/IAI.00355-17>.

**Editor** Beth McCormick, University of  
Massachusetts Medical School

**Copyright** © 2017 American Society for  
Microbiology. All Rights Reserved.

Address correspondence to Nicholas H.  
Carbonetti, [ncarbonetti@som.umaryland.edu](mailto:ncarbonetti@som.umaryland.edu).

\* Present address: Yael G. Snyder, Bacteriology  
Division, USAMRIID, Ft. Detrick, Maryland, USA.

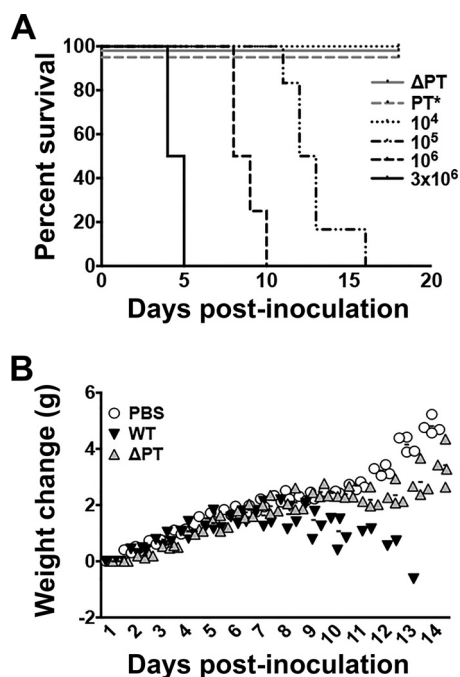


**FIG 1** Neonatal mice succumb to *B. pertussis* infection. (A) Seven-day-old C57BL/6 mice were aerosol challenged with a range of inoculation doses of the WT strain (black lines) and assessed for survival. The  $\Delta$ PT and PT\* (gray solid and dashed lines, respectively; offset for visualization) were also administered at a range of doses which were lethal for the WT but did not induce mortality (a dose of  $5 \times 10^5$  CFU/lung is depicted for each). Mice that survived past 18 dpi survived into adulthood. Survival curves represent groups of 4 or more mice from a single replicate of experiments performed at least two times. (B) Body weight was tracked daily in neonatal mice following aerosol PBS inoculation or infection with  $5 \times 10^5$  CFU/lung of the WT or  $\Delta$ PT strain and was compared with the starting weight at 1 dpi. Each data plot represents a single mouse.

are sublethal for adult (6-week-old) mice (15). However, disease pathogenesis was not studied in these mice. Those authors also found that lethality was reduced upon infection by *B. pertussis* strains with undefined transposon insertions putatively reducing secretion of pertussis toxin (PT) (15, 16). PT, a secreted virulence factor of *B. pertussis* (17), ADP-ribosylates  $G_{\alpha i}$  proteins in mammalian cells, disrupting G protein-coupled receptor (GPCR) signaling (18, 19). In adult mice, PT plays an important early role in promoting infection by inhibiting innate immune responses (20–25). However, at peak *B. pertussis* infection, PT is associated with exacerbated and prolonged lung inflammatory pathology (26, 27).

We hypothesized that *B. pertussis* infection of neonatal mice represents a model for critical pertussis in human infants and that further investigation of this model may lead to discovery of therapeutic targets for critical pertussis. We further hypothesized that PT plays a leading role contributing to neonatal pertussis disease pathogenesis and lethality. In this study, we sought to characterize *B. pertussis* infection and disease in neonatal C57BL/6 mice and determine the role of PT in pertussis pathogenesis in this model.

## RESULTS

***B. pertussis* lethality in neonatal mice is dose dependent and requires PT expression.** To establish our model, we challenged litters of 7-day-old C57BL/6 mice by aerosol with increasing doses of wild-type (WT) *B. pertussis*, an isogenic PT-deficient strain ( $\Delta$ PT), or a strain expressing an enzymatically inactive form of PT (PT\*) (23) and harvested lungs at 1 day postinoculation (dpi) to determine the challenge dose. Neonatal mice displayed 100% mortality with infectious doses of  $\geq 10^5$  WT CFU/lung. The severity of disease increased with increasing CFU, with 50% mortality at 4 dpi for a dose of  $3 \times 10^5$  CFU/lung, compared with 12 dpi for a dose of  $10^5$  CFU/lung (Fig. 1A).

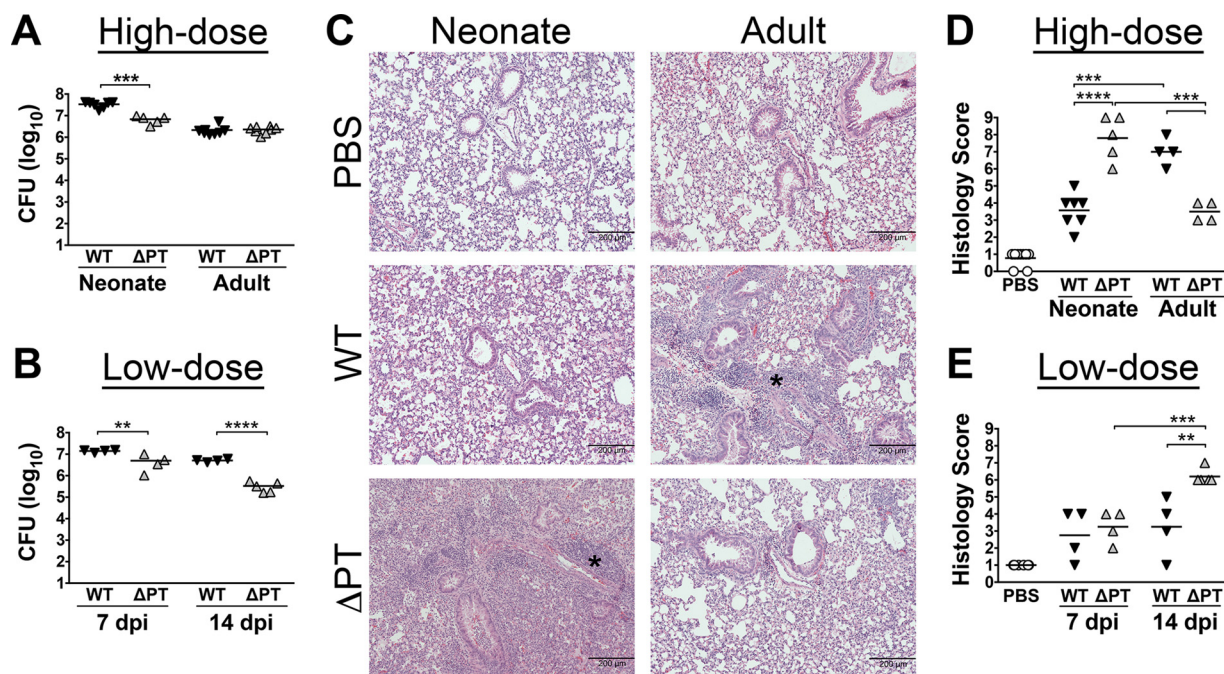


**FIG 2** Neonatal mice have increased bacterial burdens and PT-inhibited lung pathology. (A) Adult and neonatal mice inoculated with a high dose of bacteria ( $2 \times 10^6$  CFU/lung for adults and  $5 \times 10^5$  CFU/lung for neonates, as determined by lung loads at 1 dpi) were assessed for lung CFU at 7 dpi. (B) Low-dose-inoculated neonates ( $5 \times 10^4$  CFU/lung) were assessed for bacterial burden at 7 and 14 dpi. Data points represent individual animals for a single replicate of experiments performed at least two times. (C) Representative images of H&E-stained lung sections at 7 dpi following high-dose inoculation in neonatal and adult mice. An asterisk indicates the location of bronchovascular bundle (BVB) inflammation, and the scale bar represents 200  $\mu$ m. Lung pathology was scored based on the percentage of BVB involved, the degree of involvement, and the degree of lung tissue consolidation to yield a maximum score of 9. (D and E) Pathology was scored in high-dose-challenged mice at 7 dpi (D) and in low-dose-inoculated neonates at 7 dpi and 14 dpi (E). Data are representative of a single replicate of experiments performed twice. \*\*,  $P < 0.01$ ; \*\*\*,  $P < 0.001$ ; \*\*\*\*,  $P < 0.0001$ .

In contrast, 6- to 8-week-old adult C57BL/6 mice did not succumb to infection at any of these doses (data not shown). Lethality was completely dependent upon PT and its enzymatic activity, since 7-day-old mice survived infection with  $\Delta$ PT or PT\* at doses of  $5 \times 10^5$  CFU/lung, equivalent to lethal challenge with the WT, and greater (up to  $10^7$  CFU/lung) (the results from  $5 \times 10^5$  CFU/lung are depicted in Fig. 1A).

An aerosolized inoculum equivalent to a dose of  $5 \times 10^5$  CFU/lung was selected as a high-dose WT infection that was lethal for neonates (WT<sup>hi</sup>,  $\Delta$ PT<sup>hi</sup>), while a 10-fold-lower dose ( $5 \times 10^4$  CFU/lung) represented a low-dose sublethal infection (WT<sup>lo</sup>,  $\Delta$ PT<sup>lo</sup>). WT<sup>hi</sup>-infected neonatal mice gained weight at a rate equivalent to that for phosphate-buffered saline (PBS)-inoculated pups up to 7 dpi. After 7 dpi, WT<sup>hi</sup>-infected mice began to lose weight, and by 10 dpi these mice had significantly reduced weight gain compared with PBS-inoculated animals (Fig. 1B) ( $P < 0.005$ ). Weight loss correlated with disease severity, with WT<sup>hi</sup>-infected mice succumbing to infection from 10 dpi and reaching 100% mortality by 14 dpi. In contrast, weight gain in neonates inoculated with  $\Delta$ PT<sup>hi</sup> was not significantly different from that in PBS-inoculated mice (Fig. 1B). These data indicate that expression of PT during *B. pertussis* infection is required for severe disease in this model. Interestingly, pups inoculated with WT<sup>hi</sup> at 10 days of age did not display infection-induced mortality (data not shown), suggesting an age-specific impairment in the ability to survive infection.

**PT promotes *B. pertussis* colonization but inhibits airway inflammation in neonatal mice.** Multiple studies have described enhanced bacterial colonization in neonates compared with adult mice (28–30). In our study, neonatal mice displayed significantly greater lung colonization than adult mice at 7 dpi ( $P < 0.001$  for WT<sup>hi</sup> and  $P < 0.01$  for  $\Delta$ PT<sup>hi</sup>) (Fig. 2A). WT<sup>hi</sup> infection in neonates resulted in mean lung CFU of  $3.4 \times 10^7$ , compared to  $6.8 \times 10^6$  CFU/lung with  $\Delta$ PT<sup>hi</sup> ( $P < 0.001$ ), indicating that PT

promotes colonization (Fig. 2A). Neonatal mice inoculated with low doses also displayed PT-promoted lung bacterial burdens at 7 dpi, which became more pronounced at 14 dpi (Fig. 2B). The high-dose aerosol challenge in adult mice yielded a dose of  $\sim 2 \times 10^6$  CFU/lung (data not shown), similar to that used previously for intranasal inoculation (27). At 7 dpi, aerosol-inoculated adult mice did not display PT-promoted colonization (Fig. 2A).

Classical pertussis is associated with a severe paroxysmal cough in children and adults, but in infants this cough may be weak or absent (7). Since mice cannot cough, lung pathology is often assessed as a hallmark of disease severity in adult mice. We have previously described PT-associated pulmonary inflammatory histopathology and PT-enhanced cytokine production in intranasally inoculated adult mice (27). When assessing lung pathology in infected neonatal mice at 7 dpi, we were surprised to find that PT appeared to inhibit airway inflammation in these mice. In complete contrast to the case for adult mice,  $WT^{hi}$ -infected neonates displayed significantly lower levels of cellular infiltration and inflammatory cell cuffing of bronchovascular bundles (BVB) than  $\Delta PT^{hi}$ -infected neonates (Fig. 2C). This result was unexpected, as  $WT^{hi}$ -infected neonates succumb to infection, while  $\Delta PT^{hi}$ -infected neonates survive. Aerosol-inoculated adult mice replicated our previous findings of PT-enhanced inflammatory pathology (Fig. 2C). A striking age-associated difference for the role of PT in disease progression was apparent when histopathology was scored in infected neonatal mice and infected adult mice; PT inhibited pathology in neonates while promoting pathology in adult mice (Fig. 2D). Low-dose infection in neonates also displayed PT-inhibited generation of airway pathology at 14 dpi (Fig. 2E). Taken together, these results highlight the complex function of PT in infection and suggest that airway inflammatory pathology is not associated with mortality in  $WT$ -infected neonates.

In adult mice, PT has been associated with elevated and sustained expression of lung inflammatory cytokines (26, 27). In this study,  $WT^{hi}$  and  $\Delta PT^{hi}$  challenge of neonatal and adult mice resulted in significant increases in lung interleukin-1 $\beta$  (IL-1 $\beta$ ), tumor necrosis factor alpha (TNF- $\alpha$ ), and gamma interferon (IFN- $\gamma$ ) gene expression compared with those in PBS-inoculated mice at 7 dpi ( $P < 0.05$ ).  $\Delta PT^{hi}$ -infected neonatal mice had significantly higher levels of TNF- $\alpha$ , while the levels of IL-1 $\beta$  and IFN- $\gamma$  did not differ from those in  $WT^{hi}$ -infected neonates (Fig. 3A). In contrast,  $\Delta PT^{hi}$ -infected adult mice had significantly lower levels of IL-1 $\beta$  and IFN- $\gamma$  than  $WT^{hi}$ -infected adults. This result correlates well with the observed pulmonary pathology. Lung IFN- $\gamma$  expression was greater in  $WT^{hi}$ -infected adults than in  $WT^{hi}$ -infected neonates, indicating a possible impaired  $T_H1$ -type response in neonates. T cell responses are important for *B. pertussis* clearance, with protective immunity attributed to CD4 $^{+}$  but not CD8 $^{+}$  T cells (31, 32). In our model, the numbers of lung CD4 $^{+}$  and CD8 $^{+}$  T cells at 7 dpi increased with infection in neonatal and adult mice ( $P < 0.05$ ) (Fig. 3B). The ratio of CD4 $^{+}$  to CD8 $^{+}$  T cells was similar in  $WT^{hi}$ -infected and  $\Delta PT^{hi}$ -infected animals (1.8 and 1.7 for  $WT^{hi}$  in neonates and adults, respectively, versus 1.5 and 1.6 for  $\Delta PT^{hi}$  in neonates and adults, respectively), but total lung T cell numbers were significantly higher in  $\Delta PT^{hi}$ -infected mice (Fig. 3B).

#### **PT stimulates leukocytosis in neonatal mice and alters T cell phenotype.**

Leukocytosis is a hallmark of severe pertussis in infants, with high white blood cell (WBC) counts correlating significantly with pertussis-induced mortality (8). We sought to examine the contribution of PT to leukocytosis in *B. pertussis*-infected neonatal mice.  $WT^{hi}$ -infected neonatal mice displayed significantly more circulating WBC at 7 dpi than PBS-treated animals, with a marked increase ( $>6$ -fold) that was significantly greater than the modest 2-fold increase in  $\Delta PT^{hi}$ -infected mice (Fig. 4A). Comparison of neonates infected with  $WT^{lo}$  or  $\Delta PT^{lo}$  also showed PT-dependent leukocytosis at both 7 dpi and 14 dpi (Fig. 4B). In contrast, infected adult mice had no significant alteration in WBC number at 7 dpi, regardless of PT expression (Fig. 4A). This result confirms a critical role for PT in the induction of age-associated leukocytosis in pertussis.

The exact mechanism by which PT induces leukocytosis during *B. pertussis* infection is unknown (33). Expression of CD62L (L-selectin), a lymph node homing marker, was

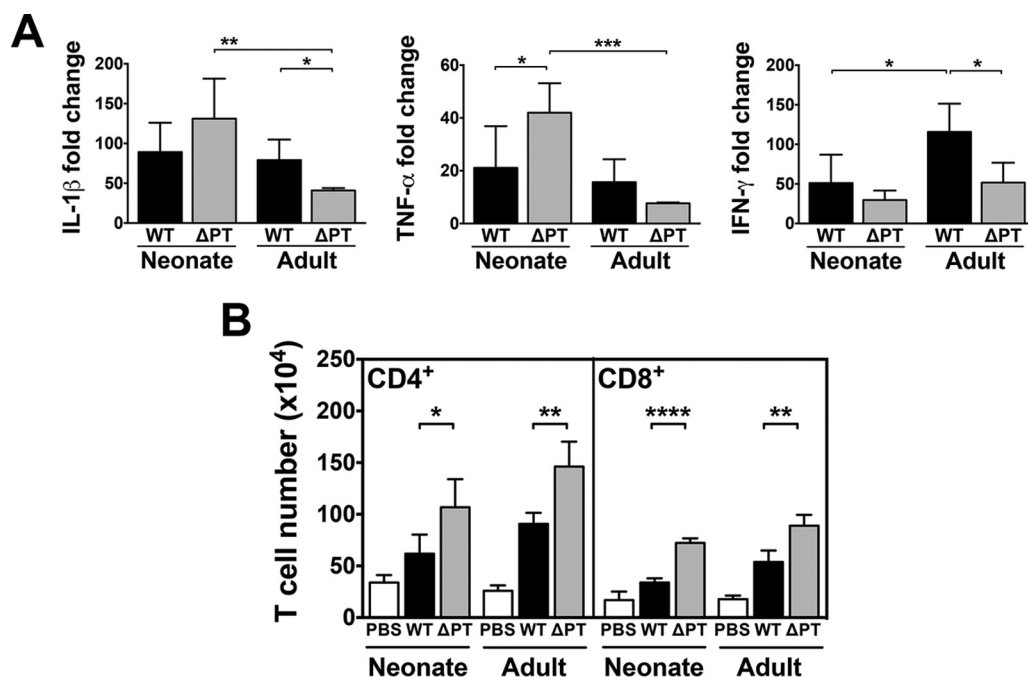


**FIG 3** *B. pertussis* infection promotes pulmonary innate cytokine production and T cell recruitment in neonatal mice. At 7 dpi with high-dose challenge, lung transcript levels of IL-1 $\beta$ , TNF- $\alpha$ , and IFN- $\gamma$  were assessed by quantitative RT-PCR (A), and total lung CD4<sup>+</sup> and CD8<sup>+</sup> T cell numbers were determined by flow cytometry following lung digest (B). Bars represent mean  $\pm$  SD for a representative experiment ( $n \geq 4$ ) performed at least two times. \*,  $P < 0.05$ ; \*\*,  $P < 0.01$ ; \*\*\*,  $P < 0.001$ ; \*\*\*\*,  $P < 0.0001$ .

significantly reduced on leukocytes from *B. pertussis*-infected human infants, suggesting a reduced capacity for leukocytes to migrate to infected tissue and peripheral lymph nodes (34). In addition, PT administered to macaques downregulated lymphocyte expression of LFA-1, an ICAM-1 binding protein involved in extravasation (35), and PT pretreatment of mouse lymphocytes inhibited LFA-1-mediated arrest on peripheral lymph node high endothelial venules (36). We therefore examined whether leukocytosis correlated with an altered T cell phenotype following high-dose infection at 7 dpi. CD62L was expressed on a lower percentage of circulating T cells in neonates than in adults in PBS-inoculated mice, and this percentage was further reduced with WT<sup>hi</sup> infection in neonatal mice (Fig. 4C), while  $\Delta$ PT<sup>hi</sup> infection in adult mice resulted in a significant increase in the percentage of CD62L<sup>+</sup> T cells (Fig. 4C). In contrast, LFA-1 was expressed on a higher percentage of neonatal circulating T cells. However, like for CD62L, LFA-1<sup>+</sup> T cell percentages were significantly lower in WT<sup>hi</sup>-infected neonates than in both PBS-inoculated and  $\Delta$ PT<sup>hi</sup>-infected mice. Consistent with the lack of leukocytosis, infection in adult mice resulted in no downregulation of either adhesion molecule tested (Fig. 4D). We next examined T cell expression of CD69, an early activation marker. Circulating CD69<sup>+</sup> T cells were reduced with WT<sup>hi</sup> and  $\Delta$ PT<sup>hi</sup> infection in neonates at 7 dpi, while the percentage of T cells expressing CD69 was increased with WT<sup>hi</sup> infection in adult mice (Fig. 4E). These data indicate that *B. pertussis* infection reduces lymphocyte adhesion marker expression in a PT-dependent manner in neonates but not in adult mice, potentially contributing to the observed leukocytosis.

#### ***B. pertussis* disseminates in neonatal mice, inducing PT-dependent pathology.**

Given that PT altered the phenotype of circulating T cells, we hypothesized that *B. pertussis* may disseminate beyond the airways in order to exert a systemic effect. Significant colonization of both the liver and spleen was observed in high-dose-inoculated neonatal mice at 7 dpi (Fig. 5A), with a dissemination index (see Materials and Methods for definition) of  $2.9 \times 10^{-4}$  for WT<sup>hi</sup> and  $1.7 \times 10^{-4}$  for  $\Delta$ PT<sup>hi</sup>. Very low levels of dissemination were detected in infected adult mice, despite the greater mass of the adult liver and spleen (dissemination index of  $2 \times 10^{-5}$  and  $3 \times 10^{-5}$  for WT<sup>hi</sup>



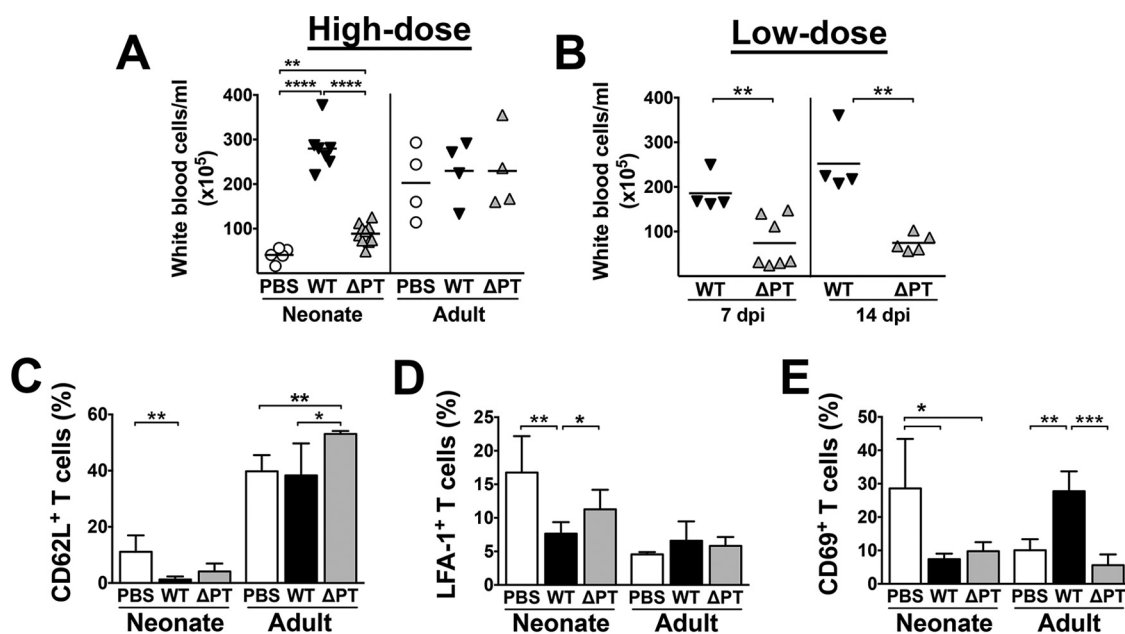


**FIG 4** PT promotes leukocytosis and downregulation of T cell adhesion molecules in neonatal mice. (A and B) Circulating WBC numbers per milliliter of blood were determined from blood harvested by cardiac puncture at 7 dpi following high-dose inoculation of neonatal or adult mice (A) or at 7 and 14 dpi for low-dose inoculated neonatal mice (B). Data points are representative of individual mice from experiments performed at least two times. (C to E) Circulating T cells were assessed for surface expression of adhesion molecules CD62L (C) and LFA-1 (D) or the early activation marker CD69 (E) by flow cytometry at 7 dpi with high-dose challenge. Bars represent mean  $\pm$  SD ( $n \geq 4$ ) for a representative experiment performed at least two times. \*,  $P < 0.05$ ; \*\*,  $P < 0.01$ ; \*\*\*,  $P < 0.001$ ; \*\*\*\*,  $P < 0.0001$ .

and  $\Delta PT^{hi}$ , respectively, at 7 dpi). In the case of both adult and neonatal infection, dissemination did not appear to be PT dependent at high doses (Fig. 5A). However, neonatal mice inoculated with  $\Delta PT^{lo}$  displayed only low-level colonization of the liver, which was cleared by 14 dpi, and failed to colonize the spleen, indicating some function of PT in promoting dissemination (Fig. 5B).  $\Delta PT^{lo}$ -infected neonates had a dissemination index of  $7 \times 10^{-5}$  at 7 dpi, compared with an index of  $18 \times 10^{-5}$  observed for  $WT^{lo}$  at the same time point. Colonization of the lungs is lowest in neonates inoculated with  $\Delta PT^{lo}$ , and so this impaired dissemination may be due to  $\Delta PT^{lo}$  not reaching a threshold level required for dissemination in this model. These organs may be colonized via the bloodstream. In our high-dose model at 7 dpi, we detected *B. pertussis* in the blood at high levels in the majority of infected neonates, while very low levels of bacteria were detected in the blood of only 50% of infected adult mice (Fig. 5C). Blood CFU were significantly greater in WT-infected than in  $\Delta PT$ -infected pups (Fig. 5C), again indicating some role for PT in dissemination.

Having observed bacterial colonization of the liver and spleen, we examined whether this dissemination was associated with pathology in these organs. Consistent with the level of colonization, high-dose-challenged adult mice displayed no altered histology in the spleen or liver (data not shown), while pathology was observed in infected neonates at 7 dpi.  $WT^{hi}$ - and  $\Delta PT^{hi}$ -infected neonates displayed sinusoidal dilation of the liver (Fig. 6A, arrows), and red blood cell congestion was also observed with  $WT^{hi}$  infection (Fig. 6A). Transcriptional analysis of neonatal livers revealed infection-induced innate cytokine upregulation (IL-1 $\beta$  and TNF- $\alpha$ ,  $P < 0.01$  compared with PBS-inoculated mice) that was reduced in the absence of PT expression, while IFN- $\gamma$  was also upregulated with infection but was not altered by the expression of PT (Fig. 6B). In the spleen,  $WT^{hi}$ -infected neonates displayed a marked reduction in white pulp (outlined in white in Fig. 6A), while the spleens of  $\Delta PT^{hi}$ -inoculated neonates displayed extensive architectural dysregulation (Fig. 6A). Despite a reduction in white pulp,  $WT^{hi}$ -infected neonates displayed increased splenic wet weight (Fig. 6C). Severe

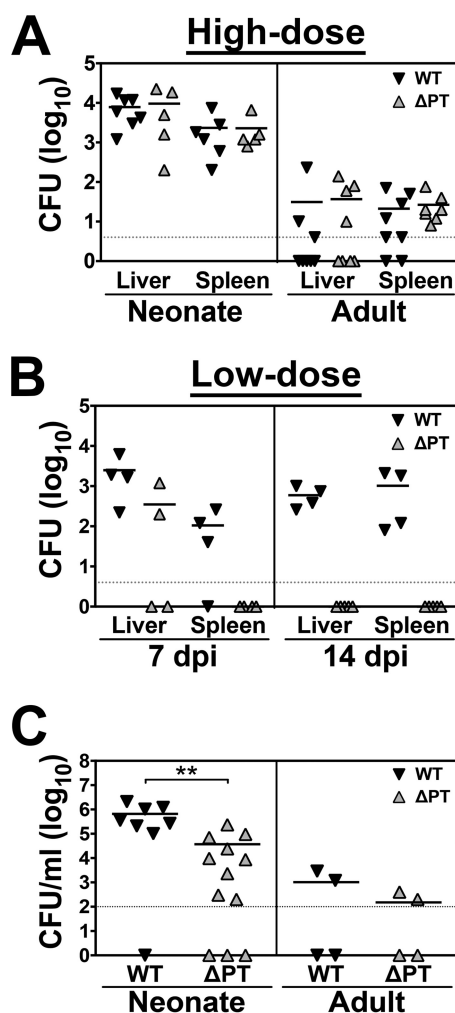


**FIG 5** *B. pertussis* dissemination is greater in infected neonatal mice than in infected adults. (A and B) Bacterial loads in the liver and spleen were assessed at 7 dpi in high-dose-challenged mice (A) or at 7 and 14 dpi for low-dose infected neonates (B). (C) The number of CFU in blood was determined at 7 dpi following high-dose challenge. Data points represent individual animals in a representative experiment performed at least two times. \*\*,  $P < 0.01$ .

neonatal pertussis is also associated with pulmonary hypertension (37). Measurement of heart rate, typically elevated with pulmonary hypertension, in high-dose-inoculated neonatal mice at 7 dpi revealed a PT-dependent increase in beats per minute (Fig. 6D).

***B. pertussis* transmission is observed in neonatal mice.** One critique of the murine model of *B. pertussis* is a lack of transmission between animals, in contrast to the very contagious nature of pertussis in humans. Transmission of a closely related pathogen, *B. bronchiseptica*, has been described in Toll-like receptor 4 (TLR4)-deficient mice (38), while a baboon model of pertussis is the only animal model described thus far in which *B. pertussis* transmission occurs (39). Given the high bacterial load in infected neonates (Fig. 2A), we hypothesized that this may result in a high degree of bacterial shedding and hence that transmission between neonatal mice may occur. Cohoused littermates were directly inoculated (index cases) or uninoculated and assessed for colonization at the day of harvest (secondary cases). High-dose-inoculated pups transmitted WT and ΔPT *B. pertussis* from index animals to all secondary cohoused littermates from 3 dpi, and this did not appear to be PT dependent (Fig. 7A). Infection appeared to be controlled in secondary animals, with no increase in bacterial burden observed from 3 dpi to 7 dpi. Low-dose infection also resulted in transmission to secondary littermates that was more efficient for WT than for ΔPT at 7 dpi (Fig. 7B).

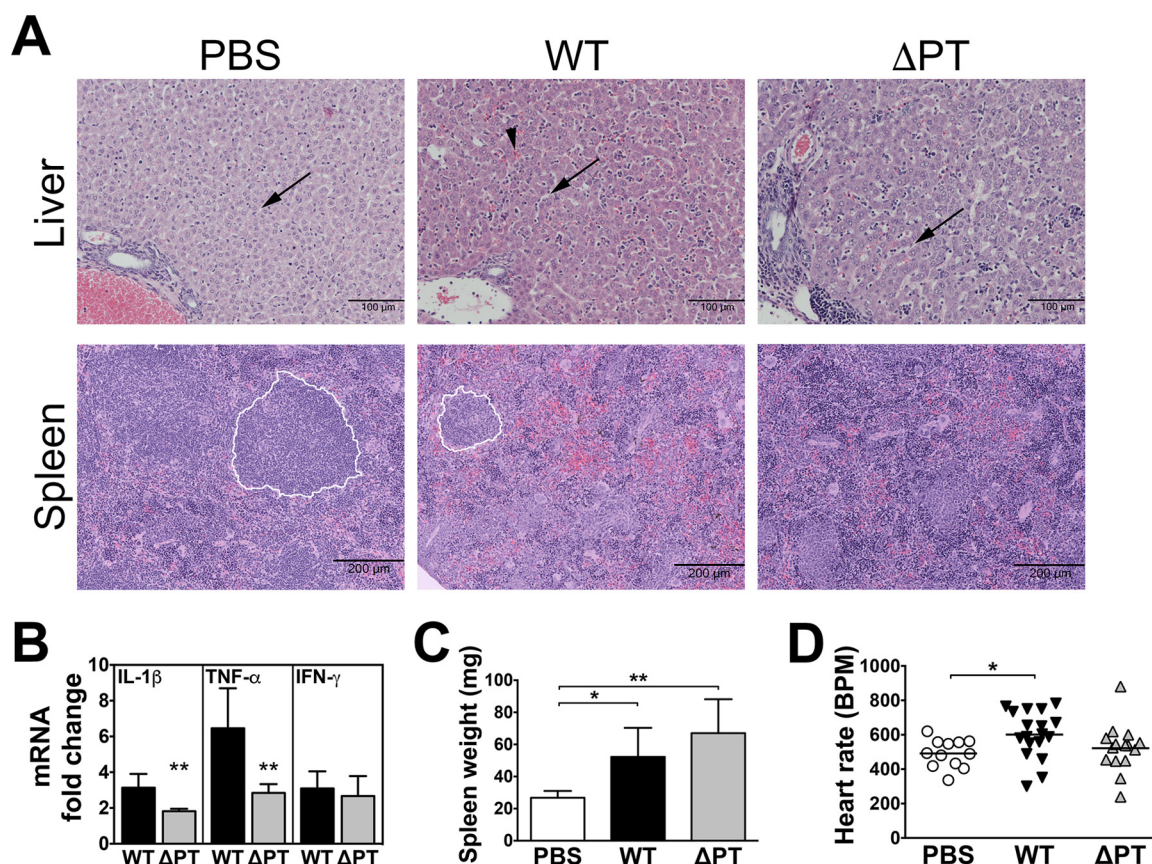


**FIG 6** PT induces systemic pathology in neonatal mice. (A) Representative images of H&E-stained liver and spleen sections from neonatal mice at 7 dpi with high-dose challenge. Arrows indicate the location of liver sinusoids, the arrowhead indicates the location of red blood cell congestion, and white lines outline splenic white pulp. Images are representative of observations from 4 mice per group. Scale bars on liver sections represent 100 μm, and scale bars on spleen sections represent 200 μm. No liver and spleen histopathology was observed in adult infected mice. (B) Liver transcript levels of IL-1β, TNF-α, and IFN-γ following high-dose inoculation of neonates were assessed at 7 dpi by quantitative RT-PCR and normalized to those for PBS-inoculated control mice. (C) Splenic wet weights were determined in neonatal mice at 7 dpi with high-dose challenge. Bars represent mean ± SD ( $n \geq 4$ ) for a representative experiment performed two times. (D) Heart rates were determined using a MouseSTAT Jr pulse oximeter and heart rate monitor in neonatal mice at 7 dpi with high-dose challenge. Data points represent individual mice, with data pooled from two replicates. \*,  $P < 0.05$ ; \*\*,  $P < 0.01$ .

Consistent with previous observations, infected adult mice did not transmit the infection to secondary adult mice; in addition, transmission from neonates to adults was not detected (data not shown). This is the first report of *B. pertussis* transmission in mice and highlights the increased susceptibility of neonates to infection.

## DISCUSSION

In this study, we have shown that the pathogenesis of *B. pertussis* infection and disease is strikingly different in neonatal versus adult mice, reflecting the more severe and sometimes fatal disease in human infants. We also showed the central role of PT in this pathogenesis. Lethality of the infection in neonatal mice was completely dependent on PT activity and yet PT inhibited lung inflammatory pathology, indicating that this is not the cause of pertussis lethality. PT promoted leukocytosis in *B. pertussis*-infected neonatal, but not adult, mice and altered circulating lymphocyte surface markers in manner similar to that seen in *B. pertussis*-infected human infants.

Age-dependent lethality of *B. pertussis* infection was previously seen in ICR mice, with 100% of 10-day-old mice succumbing to infection but only 20 to 40% of 18-day-old mice and 10 to 20% of 28-day-old mice doing so (40). Those investigators used a higher dose (aerosol inoculation with  $10^{10}$  CFU/ml for 30 min) and different mouse strain than used in our study, where we saw no lethality in 10-day-old mice inoculated at our dose ( $3 \times 10^9$  CFU/ml for 20 min). Previously, Weiss and Goodwin (15) described



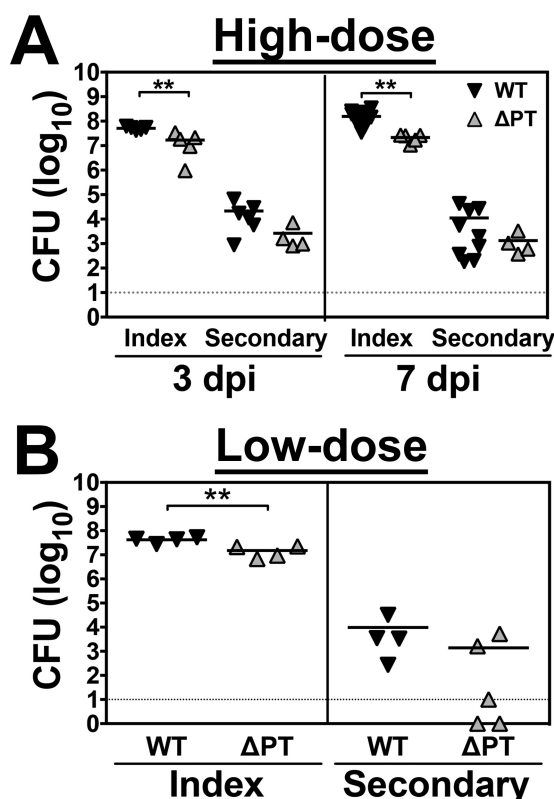


**FIG 7** Intralitter *B. pertussis* transmission occurs in neonatal mice. Index animals were directly inoculated with a high-dose or low-dose aerosol challenge and cohoused with naive “secondary” littermates. (A) Neonatal mice from the high-dose group were assessed for bacterial colonization of the lungs at 3 and 7 dpi. Data points represent individual mice, with data pooled from two replicates. (B) Colonization in the low-dose group was assessed at 7 dpi. Data points represent individual animals from a single replicate of an experiment performed twice. \*\*,  $P < 0.01$ .

reduced lethality in 6-day-old BALB/c mice infected with undefined transposon mutants of *B. pertussis* impaired in secretion of PT. Our study firmly establishes that the lethality of *B. pertussis* infection is PT dependent, since infection with the highest dose of the  $\Delta$ PT strain was not lethal.

The observed higher lung bacterial loads in WT *B. pertussis*-infected neonatal mice than in adult mice also highlight the increased susceptibility of neonatal mice to this infection, presumably due to inferior immune control. PT enhanced lung bacterial loads in neonatal mice but, surprisingly, not in aerosol-inoculated adult mice, despite our previous findings that PT enhanced lung bacterial loads in adult mice when inoculated intranasally (23, 27). It is possible that the aerosol inoculation method in adult mice delivers bacteria to different airway locations than intranasal inoculation, where the role for PT is diminished. The major surprise in this study was that there were lower levels of lung inflammatory pathology in WT *B. pertussis*-infected neonatal mice than in  $\Delta$ PT-infected neonatal mice, despite the lethality being PT dependent. This is completely opposite in adult mice. PT inhibition of lung inflammatory pathology in neonatal mice may be related to its leukocytosis-inducing effect, which is seen in neonatal but not adult mice. We hypothesize that PT is disseminated in neonatal mice and intoxicates significant numbers of circulating leukocytes, inhibiting their migration to the infected lung tissue in response to chemokines produced at the site of infection, as well as by downregulation of surface adhesion markers mediating extravasation. In contrast, PT is not disseminated in adult mice, and therefore recruitment of circulating leukocytes to infected lungs is not inhibited and hence a more severe pulmonary pathology may develop.

In addition, we saw significant bacterial dissemination from the lungs to other

organs in neonatal mice but not in adult mice, an effect that was somewhat PT dependent. This bacterial dissemination may explain, or at least contribute to, the dissemination of PT, and pathology in these other organs was also PT dependent. There are limited data on the effect of *B. pertussis* infection on organs beyond the lungs in humans; however, one publication describes liver and spleen pathology similar to that observed here in a 16-day-old male who died as a result of critical pertussis (41). Interestingly, we recently showed that treatment of *B. pertussis*-infected neonatal mice with a sphingosine-1-phosphate receptor agonist significantly reduced lethality, and this effect correlated with reduction in bacterial dissemination but not in leukocytosis (42). Therefore, dissemination of the bacterial infection and the pathological effects of disseminated PT may be the predominant cause of lethality in this model. We saw a significant increase in heart rate associated with PT in the infected neonatal mice, and the liver sinusoidal dilation observed in this model may be a sign of heart failure (43), suggesting that effects of PT on core physiological functions may be the ultimate cause of lethality in pertussis.

The factors involved in *B. pertussis* transmission are poorly understood, largely due to the limited availability of a low-cost animal model. To date, baboons are the only animals in which *B. pertussis* transmission has been described (39), but this is an expensive model and hence not suitable for screening studies. In this study, we describe transmission of *B. pertussis* in the mouse for the first time. The neonatal mouse model of transmission will provide a platform to investigate virulence genes associated with transmission and may be useful for investigating vaccine efficacy following maternal immunization and developing infant-targeted vaccines against *B. pertussis*. Here, we show that one virulence factor, PT, has a limited role in *B. pertussis* transmission.

An important question is to what extent the neonatal mouse model of *B. pertussis* infection recapitulates severe pertussis disease in human infants. The vast majority of fatal cases of pertussis are in young infants (4, 9), which correlates well with the age-dependent lethality of the mouse model. We observed higher lung bacterial loads in neonatal mice than in adult mice, and in humans, one study found evidence of higher bacterial loads in nasopharyngeal swabs from *B. pertussis*-infected infants than in those from adults (44). Leukocytosis is observed in pertussis infections only in young children and not in infected adolescents and adults (33, 45, 46), a scenario identical to that in the mouse model. Phenotypic changes in circulating naive T lymphocytes (which may contribute to leukocytosis) observed in blood from infants with pertussis (34, 47) were also seen in our infected neonatal mice (Fig. 4). Human lung inflammatory pathology associated with *B. pertussis* infection has been assessed only from autopsy studies of fatal cases in infants. These studies show necrotizing bronchitis, alveolar epithelial damage and hemorrhage, and fibrinous edema (6, 10). Although we did not perform extensive pathology analysis of our mice, several of these pathology findings were apparent in *B. pertussis*-infected neonatal mice (Fig. 2). However, dissemination of *B. pertussis* infection beyond the respiratory tract, observed here in our infected neonatal mice, is not reported in human infant pertussis cases. There are rare reports of pertussis bacteremia detected in adults with other serious health conditions (48, 49). Although to our knowledge there are no reports of disseminated pertussis infection in infants, routine culture of blood samples for *B. pertussis* before antibiotic treatment is not typically performed, and so disseminated infection may have been missed. Overall, we believe that the neonatal mouse model recapitulates many aspects of pertussis in human infants and will therefore be a useful model for further investigation of severe pertussis pathogenesis and potential therapeutic treatments for this age group.

## MATERIALS AND METHODS

**Bacterial strains.** The WT (Tohama-derived),  $\Delta$ PT (isogenic PT-deficient mutant), and PT\* (isogenic mutant producing enzymatically inactive PT) *B. pertussis* strains (23) were grown on Bordet-Gengou (BG) agar plates supplemented with 10% defibrinated sheep blood and 200  $\mu$ g/ml streptomycin.

**Mouse infections.** Seven-day-old and 6- to 8-week-old C57BL/6 mice (Charles River) were used in accordance with the University of Maryland, Baltimore (UMB), Institutional Animal Care and Use Com-

**TABLE 1** Primers used in this study

Gene	Primer sequence	
	Forward	Reverse
HPRT	5'-GCTGACCTGCTGGATTACATTAA-3'	5'-GATCATTACAGTAGCTCTTCAGTCTG-3'
IL-1 $\beta$	5'-TGTGAAATGCCACCTTTTGA-3'	5'-GGTCAAAGGTTTGAAGCAG-3'
TNF- $\alpha$	5'-CCACGTCGTAGCAAACACC-3'	5'-CGGCTGGCACCAGTGTG-3'
IFN- $\gamma$	5'-GGAGGAACCTGGCAAAAGGATG-3'	5'-GACGCTTATGTTGTTGCTGATGG-3'

mittee. Bacterial inocula were prepared in PBS, and the inoculum was administered via a nebulizer system (Pari Vios) for 20 min. The dissemination index was calculated by summing the total CFU in the livers and spleens in each group and dividing by the total lung CFU for that respective group. For transmission studies, 4 pups were directly inoculated and cohoused with  $\geq 4$  naive littermates. Heart rates were determined using a MouseSTAT Jr pulse oximeter and heart rate monitor (Kent Scientific). Leukocytosis was determined from blood acquired by cardiac puncture and treated with ammonium chloride-potassium (ACK) lysis buffer. Left lung, liver sections, and spleen were fixed in 10% (wt/vol) formalin, mounted, and hematoxylin and eosin (H&E) stained by the UMB Pathology EM and Histology Laboratory. Pulmonary histopathology was scored based on BVB inflammation and cellular infiltration as previously described (50).

**RNA processing.** RNA was isolated using TRIzol reagent (Invitrogen) and reverse transcribed using a reverse transcription system (Promega) as per the manufacturer's instructions. Quantitative real-time PCR (RT-PCR) was performed with Maxima SYBR green/ROX qPCR master mix (Thermo Scientific) in an Applied Biosystems 7500 Fast real-time PCR system. Transcript levels of cytokine genes were normalized to the hypoxanthine phosphoribosyltransferase (HPRT) housekeeping gene (primer sequences are given in Table 1) and compared with those from PBS-inoculated age-matched mice (calculated by  $2^{-\Delta\Delta CT}$ ).

**Flow cytometry.** Blood was treated with ACK, and lungs were digested for flow cytometry (51). Cells ( $10^6$ /sample) were labeled with peridinin chlorophyll protein (PerCP)-eFluor710-anti-CD3, phycoerythrin (PE)-anti-CD4, allophycocyanin (APC)/Cy7-anti-CD8a, Pacific Blue-anti-CD62L, PE-anti-LFA-1, and APC/Cy7-anti-CD69 and analyzed using a BD LSRII flow cytometer.

**Statistical analysis.** All plots represent the mean  $\pm$  standard deviation (SD). Significance was determined by the *t* test for 2-group analyses and by analysis of variance (ANOVA) and the Kruskal-Wallis test for 3 or more groups. Significance was determined for survival curves by the log rank (Mantel-Cox) test.

## ACKNOWLEDGMENTS

This work was supported by the National Institute of Allergy and Infectious Diseases, National Institutes of Health (grant numbers AI117095 and AI101055).

We thank other members of the Carbonetti lab and members of Marcela Pasetti's lab for their assistance with this work.

## REFERENCES

1. Tan T, Dalby T, Forsyth K, Halperin SA, Heininger U, Hozbor D, Plotkin S, Ulloa-Gutierrez R, Wirsing von Konig CH. 2015. Pertussis across the globe: recent epidemiologic trends from 2000 to 2013. *Pediatr Infect Dis J* 34:e222–e232. <https://doi.org/10.1097/INF.0000000000000795>.
2. Kilgore PE, Salim AM, Zervos MJ, Schmitt HJ. 2016. Pertussis: microbiology, disease, treatment, and prevention. *Clin Microbiol Rev* 29:449–486. <https://doi.org/10.1128/CMR.00083-15>.
3. Salim AM, Liang Y, Kilgore PE. 2015. Protecting newborns against pertussis: treatment and prevention strategies. *Paediatr Drugs* 17: 425–441. <https://doi.org/10.1007/s40272-015-0149-x>.
4. Tiwari TS, Baughman AL, Clark TA. 2015. First pertussis vaccine dose and prevention of infant mortality. *Pediatrics* 135:990–999. <https://doi.org/10.1542/peds.2014-2291>.
5. Berger JT, Carcillo JA, Shanley TP, Wessel DL, Clark A, Holubkov R, Meert KL, Newth CJ, Berg RA, Heidemann S, Harrison R, Pollack M, Dalton H, Harvill E, Karanikas A, Liu T, Burr JS, Doctor A, Dean JM, Jenkins TL, Nicholson CE, Eunice Kennedy Shriver National Institute of Child Health and Human Development (NICHD) Collaborative Pediatric Critical Care Research Network (CPCCRN). 2013. Critical pertussis illness in children: a multicenter prospective cohort study. *Pediatr Crit Care Med* 14:356–365. <https://doi.org/10.1097/PCC.0b013e31828a70fe>.
6. Sawal M, Cohen M, Irazuzta JE, Kumar R, Kirton C, Brundler MA, Evans CA, Wilson JA, Raffeeq P, Azaz A, Rotta AT, Vora A, Vohra A, Abboud P, Mirkin LD, Cooper M, Dishop MK, Graf JM, Petros A, Klonin H. 2009. Fulminant pertussis: a multi-center study with new insights into the clinico-pathological mechanisms. *Pediatr Pulmonol* 44:970–980. <https://doi.org/10.1002/ppul.21082>.
7. Rocha G, Soares P, Soares H, Pissarra S, Guimaraes H. 2015. Pertussis in the newborn: certainties and uncertainties in 2014. *Paediatr Respir Rev* 16:112–118. <https://doi.org/10.1016/j.prrv.2014.01.004>.
8. Winter K, Zipprich J, Harriman K, Murray EL, Gornbein J, Hammer SJ, Yeganeh N, Adachi K, Cherry JD. 2015. Risk factors associated with infant deaths from pertussis: a case-control study. *Clin Infect Dis* 61:1099–1106. <https://doi.org/10.1093/cid/civ472>.
9. Chow MY, Khandaker G, McIntyre P. 2016. Global childhood deaths from pertussis: a historical review. *Clin Infect Dis* 63:S134–S141. <https://doi.org/10.1093/cid/ciw529>.
10. Paddock CD, Sanden GN, Cherry JD, Gal AA, Langston C, Tatti KM, Wu KH, Goldsmith CS, Greer PW, Montague JL, Eliason MT, Holman RC, Guarner J, Shieh WJ, Zaki SR. 2008. Pathology and pathogenesis of fatal *Bordetella pertussis* infection in infants. *Clin Infect Dis* 47:328–338. <https://doi.org/10.1086/589753>.
11. Scanlon KM, Skerry C, Carbonetti NH. 2015. Novel therapies for the treatment of pertussis disease. *Pathog Dis* 73:ftv074. <https://doi.org/10.1093/femspd/ftv074>.
12. Adkins B, Leclerc C, Marshall-Clarke S. 2004. Neonatal adaptive immunity comes of age. *Nat Rev Immunol* 4:553–564. <https://doi.org/10.1038/nri1394>.
13. Levy O. 2007. Innate immunity of the newborn: basic mechanisms and clinical correlates. *Nat Rev Immunol* 7:379–390. <https://doi.org/10.1038/nri2075>.

14. Basha S, Surendran N, Pichichero M. 2014. Immune responses in neonates. *Expert Rev Clin Immunol* 10:1171–1184. <https://doi.org/10.1586/1744666X.2014.942288>.
15. Weiss AA, Goodwin MS. 1989. Lethal infection by *Bordetella pertussis* mutants in the infant mouse model. *Infect Immun* 57:3757–3764.
16. Goodwin MS, Weiss AA. 1990. Adenylate cyclase toxin is critical for colonization and pertussis toxin is critical for lethal infection by *Bordetella pertussis* in infant mice. *Infect Immun* 58:3445–3447.
17. Carbonetti NH. 2015. Contribution of pertussis toxin to the pathogenesis of pertussis disease. *Pathog Dis* 73:ftv073. <https://doi.org/10.1093/femspd/ftv073>.
18. Carbonetti NH. 2010. Pertussis toxin and adenylate cyclase toxin: key virulence factors of *Bordetella pertussis* and cell biology tools. *Future Microbiol* 5:455–469. <https://doi.org/10.2217/fmb.09.133>.
19. Coutte L, Loch C. 2015. Investigating pertussis toxin and its impact on vaccination. *Future Microbiol* 10:241–254. <https://doi.org/10.2217/fmb.14.123>.
20. Andreasen C, Carbonetti NH. 2008. Pertussis toxin inhibits early chemokine production to delay neutrophil recruitment in response to *Bordetella pertussis* respiratory tract infection in mice. *Infect Immun* 76:5139–5148. <https://doi.org/10.1128/IAI.00895-08>.
21. Carbonetti NH. 2007. Immunomodulation in the pathogenesis of *Bordetella pertussis* infection and disease. *Curr Opin Pharmacol* 7:272–278. <https://doi.org/10.1016/j.coph.2006.12.004>.
22. Carbonetti NH, Artamonova GV, Andreasen C, Bushar N. 2005. Pertussis toxin and adenylate cyclase toxin provide a one-two punch for establishment of *Bordetella pertussis* infection of the respiratory tract. *Infect Immun* 73:2698–2703. <https://doi.org/10.1128/IAI.73.5.2698-2703.2005>.
23. Carbonetti NH, Artamonova GV, Mays RM, Worthington ZE. 2003. Pertussis toxin plays an early role in respiratory tract colonization by *Bordetella pertussis*. *Infect Immun* 71:6358–6366. <https://doi.org/10.1128/IAI.71.11.6358-6366.2003>.
24. Carbonetti NH, Artamonova GV, Van Rooijen N, Ayala VI. 2007. Pertussis toxin targets airway macrophages to promote *Bordetella pertussis* infection of the respiratory tract. *Infect Immun* 75:1713–1720. <https://doi.org/10.1128/IAI.01578-06>.
25. Kirimanjesswara GS, Agosto LM, Kennett MJ, Bjornstad ON, Harvill ET. 2005. Pertussis toxin inhibits neutrophil recruitment to delay antibody-mediated clearance of *Bordetella pertussis*. *J Clin Invest* 115:3594–3601. <https://doi.org/10.1172/JCI24609>.
26. Andreasen C, Powell DA, Carbonetti NH. 2009. Pertussis toxin stimulates IL-17 production in response to *Bordetella pertussis* infection in mice. *PLoS One* 4:e7079. <https://doi.org/10.1371/journal.pone.0007079>.
27. Connelly CE, Sun Y, Carbonetti NH. 2012. Pertussis toxin exacerbates and prolongs airway inflammatory responses during *Bordetella pertussis* infection. *Infect Immun* 80:4317–4332. <https://doi.org/10.1128/IAI.00808-12>.
28. Fitzpatrick EA, You D, Shrestha B, Siefker D, Patel VS, Yadav N, Jaligama S, Cormier SA. 2017. A neonatal murine model of MRSA pneumonia. *PLoS One* 12:e0169273. <https://doi.org/10.1371/journal.pone.0169273>.
29. Siegel SJ, Tamashiro E, Weiser JN. 2015. Clearance of pneumococcal colonization in infants is delayed through altered macrophage trafficking. *PLoS Pathog* 11:e1005004. <https://doi.org/10.1371/journal.ppat.1005004>.
30. Elahi S, Ertelt JM, Kinder JM, Jiang TT, Zhang X, Xin L, Chaturvedi V, Strong BS, Qualls JE, Steinbrecher KA, Kalfa TA, Shaaban AF, Way SS. 2013. Immunosuppressive CD71+ erythroid cells compromise neonatal host defence against infection. *Nature* 504:158–162. <https://doi.org/10.1038/nature12675>.
31. Mills KH, Barnard A, Watkins J, Redhead K. 1993. Cell-mediated immunity to *Bordetella pertussis*: role of Th1 cells in bacterial clearance in a murine respiratory infection model. *Infect Immun* 61:399–410.
32. Leef M, Elkins KL, Barbic J, Shahin RD. 2000. Protective immunity to *Bordetella pertussis* requires both B cells and CD4(+) T cells for key functions other than specific antibody production. *J Exp Med* 191:1841–1852. <https://doi.org/10.1084/jem.191.11.1841>.
33. Carbonetti NH. 2016. Pertussis leukocytosis: mechanisms, clinical relevance and treatment. *Pathog Dis* <https://doi.org/10.1093/femspd/ftw087>.
34. Hodge G, Hodge S, Markus C, Lawrence A, Han P. 2003. A marked decrease in L-selectin expression by leucocytes in infants with *Bordetella pertussis* infection: leucocytosis explained? *Respirology* 8:157–162. <https://doi.org/10.1046/j.1440-1843.2003.00459.x>.
35. Schenkel AR, Pauza CD. 1999. Pertussis toxin treatment in vivo reduces surface expression of the adhesion integrin leukocyte function antigen-1 (LFA-1). *Cell Adhes Commun* 7:183–193. <https://doi.org/10.3109/15419069909010801>.
36. Warnock RA, Askari S, Butcher EC, von Andrian UH. 1998. Molecular mechanisms of lymphocyte homing to peripheral lymph nodes. *J Exp Med* 187:205–216. <https://doi.org/10.1084/jem.187.2.205>.
37. Donoso A, Leon J, Ramirez M, Rojas G, Oberpaur B. 2005. Pertussis and fatal pulmonary hypertension: a discouraged entity. *Scand J Infect Dis* 37:145–148. <https://doi.org/10.1080/00365540510026436>.
38. Rolin O, Smalridge W, Henry M, Goodfield L, Place D, Harvill ET. 2014. Toll-like receptor 4 limits transmission of *Bordetella bronchiseptica*. *PLoS One* 9:e85229. <https://doi.org/10.1371/journal.pone.0085229>.
39. Warfel JM, Beren J, Merkel TJ. 2012. Airborne transmission of *Bordetella pertussis*. *J Infect Dis* 206:902–906. <https://doi.org/10.1093/infdis/jis443>.
40. Sato Y, Izumiya K, Sato H, Cowell JL, Manclark CR. 1980. Aerosol infection of mice with *Bordetella pertussis*. *Infect Immun* 29:261–266.
41. Torre JA, Benevides GN, de Melo AM, Ferreira CR. 2015. Pertussis: the resurgence of a public health threat. *Autops Case Rep* 5:9–16.
42. Skerry C, Scanlon K, Ardanuy J, Roberts D, Zhang L, Rosen H, Carbonetti NH. 2017. Reduction of pertussis inflammatory pathology by therapeutic treatment with sphingosine-1-phosphate receptor ligands by a pertussis toxin-insensitive mechanism. *J Infect Dis* 215:278–286. <https://doi.org/10.1093/infdis/jiw536>.
43. Louie CY, Pham MX, Daugherty TJ, Kambham N, Higgins JP. 2015. The liver in heart failure: a biopsy and explant series of the histopathologic and laboratory findings with a particular focus on pre-cardiac transplant evaluation. *Mod Pathol* 28:932–943. <https://doi.org/10.1038/modpathol.2015.40>.
44. Nakamura Y, Kamachi K, Toyozumi-Ajisaka H, Otsuka N, Saito R, Tsu-ruoka J, Katsuta T, Nakajima N, Okada K, Kato T, Arakawa Y. 2011. Marked difference between adults and children in *Bordetella pertussis* DNA load in nasopharyngeal swabs. *Clin Microbiol Infect* 17:365–370. <https://doi.org/10.1111/j.1469-0691.2010.03255.x>.
45. Aoyama T, Takeuchi Y, Goto A, Iwai H, Murase Y, Iwata T. 1992. Pertussis in adults. *Am J Dis Child* 146:163–166.
46. Heininger U, Klich K, Stehr K, Cherry JD. 1997. Clinical findings in *Bordetella pertussis* infections: results of a prospective multicenter surveillance study. *Pediatrics* 100:E10.
47. Hudnall SD, Molina CP. 2000. Marked increase in L-selectin-negative T cells in neonatal pertussis. The lymphocytosis explained? *Am J Clin Pathol* 114:35–40. <https://doi.org/10.1309/BANX-8JKM-TUQN-4D6P>.
48. Janda WM, Santos E, Stevens J, Celig D, Terrile L, Schreckenberger PC. 1994. Unexpected isolation of *Bordetella pertussis* from a blood culture. *J Clin Microbiol* 32:2851–2853.
49. Troseld M, Jonassen TO, Steinbakk M. 2006. Isolation of *Bordetella pertussis* in blood culture from a patient with multiple myeloma. *J Infect* 52:e11–e13. <https://doi.org/10.1016/j.jinf.2005.04.014>.
50. Scanlon KM, Gau Y, Zhu J, Skerry C, Wall SM, Soleimani M, Carbonetti NH. 2014. Epithelial anion transporter pendrin contributes to inflammatory lung pathology in mouse models of *Bordetella pertussis* infection. *Infect Immun* 82:4212–4221. <https://doi.org/10.1128/IAI.02222-14>.
51. Nakano H, Cook DN. 2013. Pulmonary antigen presenting cells: isolation, purification, and culture. *Methods Mol Biol* 1032:19–29. [https://doi.org/10.1007/978-1-62703-496-8\\_2](https://doi.org/10.1007/978-1-62703-496-8_2).